# Gamow-Teller Strengths of the Inverse-Beta Transition $^{176}$Yb→$^{176}$Lu for Spectroscopy of Proton-Proton and other sub-MeV Solar Neutrinos

M. Fujiwara,[1,2] H. Akimune,[3] A.M. van den Berg,[4] M. Cribier,[5] I. Daito,[6] H. Ejiri,[1] H. Fujimura,[1] Y. Fujita,[6] C.D. Goodman,[8] K. Hara,[1] M.N. Harakeh,[4] F. Ihara,[1] T. Ishikawa,[9] J. Jänecke,[10] T. Kawabata,[9] R.S. Raghavan,[11] K. Schwarz,[1] M. Tanaka,[12] T. Yamanaka,[1] M. Yosoi,[1] and R.G.T. Zegers[2,4]

[1] *Research Center for Nuclear Physics, Osaka University, Mihogaoka 10-1, Ibaraki, Osaka 657-0047, Japan*
[2] *Advanced Science Research Center, JAERI, Tokai, Ibaraki, 319-1195 Japan*
[3] *Konan University, Higashinada, Kobe 658, Japan*
[4] *Kernfysisch Versneller Instituut, 9747 AA Groningen, The Netherlands*
[5] *CEA/Saclay, DAPNIA/SPP 91191 Gif-sur-Yvette Cedex, France*
[6] *Nagoya University, Department of Physics, 464 Nagoya, Japan*
[7] *Department of Physics, Osaka University, 560-0043, Japan*
[8] *Indiana University Cyclotron Facility, Bloomington, Indiana, USA*
[9] *Department of Physics, Kyoto University, Kyoto 606-8502, Japan*
[10] *Department of Physics, University of Michigan, Ann Arbor, MI 48109-1120, USA*
[11] *Bell Laboratories, Lucent Technologies, Murray Hill, New Jersey 07974, U.S.A.*
[12] *Kobe Tokiwa Jr. College, Nagata 653, Japan*

(June 6, 2000)

Discrete Gamow-Teller (GT) transitions, $^{176}$Yb→$^{176}$Lu at low excitation energies have been measured via the ($^3$He,$t$) reaction at 450 MeV and at 0°. For $^{176}$Yb, two low-lying states are observed, setting low thresholds Q($\nu$)=301 and 445 keV for neutrino ($\nu$) capture. Capture rates estimated from the measured GT strengths, the simple two-state excitation structure, and the low Q($\nu$) in Yb–Lu indicate that Yb-based $\nu$-detectors are well suited for a direct measurement of the complete sub-MeV solar electron-neutrino ($\nu_e$) spectrum (including *pp* neutrinos) where definitive effects of flavor conversion are expected.

26.65.+t, 25.55.Kr, 27.70.+q

The major result of experimental solar-neutrino research to date shows that the observed fluxes of solar neutrinos are much reduced compared with theoretical predictions based on the standard solar model (SSM) [1]. Particularly sharp questions are posed by the results from the Gallex [2] and Sage [3] experiments at the low-energy end of the spectrum (from the $p+p$, $^7$Be and CNO reactions in the sun) that are in contrast with those from Super-Kamiokande at high energies (from the decay of $^8$B) [4]. The low-energy results imply a negligible flux of $^7$Be neutrinos which is inconsistent with the observed sizeable flux of high-energy $^8$B neutrinos because the $^8$B activity in the sun cannot arise without the precursor $^7$Be in the reaction $^7$Be+$p$→$^8$B. These results suggest mechanisms beyond possible astrophysical shortcomings of the SSM. The only other possibility is non-standard neutrino physics, viz. the conversion of the original electron-flavor solar neutrinos ($\nu_e$) to undetected $\mu$ and $\tau$ flavors. Evidence for $\nu_\mu$–$\nu_\tau$ flavor conversion has recently been observed by Super-Kamiokande [5].

The conceivable conversion mechanisms produce $\nu_e$ flux deficits that are energy dependent (typically strongest at low energies) and result in large deficits of either the *pp* and/or the $^7$Be $\nu_e$ fluxes, the two dominant features of the sub-MeV spectrum. A deficit in the model-independent *pp*-neutrino flux and/or a $^7$Be $\nu_e$ flux measurably smaller than the total all-flavor flux (expected from the Borexino experiment [6] in particular), would provide the most direct proof of flavor conversion. A real-time measurement of the complete $\nu_e$ spectrum from the sun and source-specific fluxes is, thus, of central interest for solving the solar-$\nu$ problem. Such data are not available yet since the operating low-energy Ga detectors yield only the integral signal rate above a threshold, not the fluxes from specific solar $\nu$ sources.

Recently, Raghavan [7] suggested a possible way to construct a low-threshold, flavor-specific scheme for real-time detection of solar neutrinos via neutrino captures based on the charged current mediated Gamow-Teller (GT) transitions $\nu_e$+$^{176}$Yb→$e^-$ + $^{176}$Lu$^*$ and $\nu_e$+$^{160}$Gd→$e^-$ + $^{160}$Tb$^*$. The basic idea is to identify absorption events of *pp* and $^7$Be neutrinos by a delayed coincidence between a prompt $e^-$ event and a cascade $\gamma$-ray via isomeric states in $^{176}$Lu or $^{160}$Tb. The coincidence tag (with time gates $\leq 10^{-7}$ s) allows suppression of background events by a factor of $10^7$. For the first time, this scheme offers the tools for practical real-time spectroscopy even of *pp*–neutrinos despite the formidable backgrounds that have precluded low-energy $\nu$ spectroscopy so far. Feasibility studies are in progress for constructing such a solar $\nu$ detector LENS (Low-Energy Neutrino Spectroscopy) [8].

The basic input data for designing LENS are the cross sections of the GT transitions in Yb and Gd for which the weak matrix elements B(GT) must be determined for each of the low-lying $1^+$ states excited by neutrino cap-

ture. The low energy-excitations in Yb-Lu and Gd-Tb consist of several close-lying known $1^+$ states. Clarification of the states relevant to LENS thus requires high-resolution spectra. We have therefore measured high resolution ($^3$He,$t$) spectra at 0° using a $^3$He beam at 450 MeV. This work complements a different approach to find B(GT) via $(p,n)$ measurements [9] on the same targets.

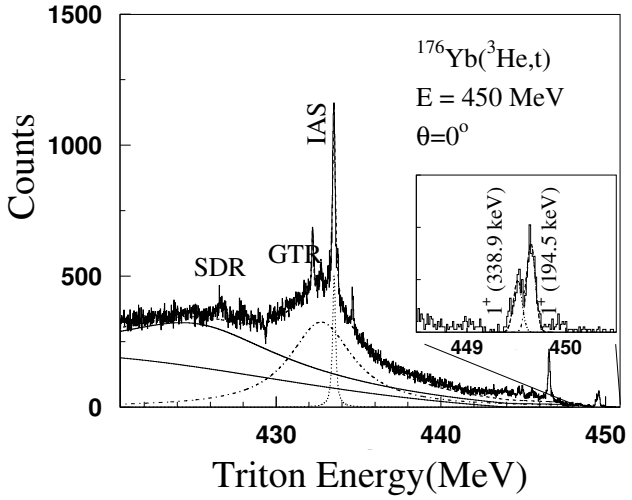


FIG. 1. Triton energy spectrum from the $^{176}$Yb($^3$He,$t$) reaction at 0° taken with a $^3$He beam of 150 A·MeV. A sharp IAS peak and two broad bumps corresponding to the Gamow-Teller resonance (GTR), and the spin dipole resonance (SDR) are observed. The global structure of the spectrum is fitted by assuming an underlying continuum due to quasi-free scattering. Discrete states at the low excitation energy are displayed in the expanded inset. Sharp peaks near to IAS are due to C and O contaminations

The ($^3$He,$t$) reaction at 450 MeV has already been demonstrated to be useful in getting the B(GT) values. Since the full Fermi transition strength B(F)=N–Z is exhausted by the isobaric analog state (IAS), the B(GT) values can be obtained from the singles ($^3$He,$t$) spectra by using the ratio of the cross sections to the $1^+$ states and the IAS [10]. The measurements described below show that the B(GT) values obtained here can be used reliably to estimate solar neutrino rates in LENS.

The ($^3$He,$t$) experiment was performed at E($^3$He)=450 MeV at the RCNP cyclotron facility of Osaka University using the spectrometer Grand Raiden [11] which was set at $\theta = 0°$ with a solid angle of $\Delta\Omega = 1.6$ msr. Both the incident $^3$He$^{++}$ beam and the reaction products entered into the spectrometer set at 0°. A metallic target of $^{176}$Yb (96.7 % enrichment, 3.3 mg/cm$^2$) was used. The $^3$He$^{++}$ beam, which has a much small magnetic rigidity than the tritons,was stopped at the internal Faraday cup in the first dipole (D1) magnet. Details of the experimental setup are described in Ref. [11]. Particles analyzed by the spectrometer were detected in the focal-plane detection system consisting of two multi–wire drift chambers (MWDC's) and two ΔE plastic scintillation counters, whose signals were used for particle identification as well as for triggering the events. The MWDC's gave information on the arrival positions at the focal plane and the scattering angles of the tritons.

Very good identification with the focal-plane detector of the spectrograph was required to overcome the huge background due to the $^3$He$^{++} \rightarrow {}^3$He$^+$ atomic charge-exchange process [12], since the Q-values for the ($^3$He,$t$) reactions on $^{176}$Yb leading to the lowest $1^+$ states in the residual nuclei is $\leq 0.3$ MeV. For this purpose, we added a plastic scintillation counter with a thickness of 1 mm in front of the two $\Delta E$ counters of 10 mm thickness for improved particle identification. This front counter should be very thin to avoid creating tritons induced by ($^3$He,$t$) reactions in the scintillator itself. With this technique, we could obtain a spectrum free from the $^3$He$^{++} \rightarrow {}^3$He$^+$ atomic charge-exchange process.

To achieve a high energy resolution of around 100 keV, we installed an energy defining slit in the beam-transport system from the K=400 MeV ring cyclotron to the target position. The image-defining slit was set at the first beam-focusing position of the beam-line. The technique of dispersion matching between the beam-line and the spectrometer was employed to obtain the required high resolution. An overall energy resolution of $\Delta E = 100\sim140$ keV was obtained, which was sufficient to resolve the low-lying $1^+$ states in $^{176}$Lu.

TABLE I. Gamow-Teller and Fermi strengths B(GT) and B(F) of the levels observed in the $^{176}$Yb($^3$He,$t$)$^{176}$Lu and $^{160}$Gd($^3$He,$t$)$^{160}$Tb reactions.

| $^{176}_{70}$Yb$_{106}$($^3$He,$t$)$^{176}_{71}$Lu$_{105}$ | | |
|---|---|---|
| $J^\pi$ | $E_x$(keV) | B(GT) or B(F) |
| $1^+_1$ | 194.5 | 0.20±0.04 |
| $1^+_2$ | 338.9 | 0.11±0.02 |
| $1^+_3$ | 3070 | 0.62±0.08 |
| $0^+_{IAS}$ | 16026 ± 6 | 36 |
| $^{160}_{64}$Gd$_{96}$($^3$He,$t$)$^{160}_{65}$Tb$_{95}$ | | |
| $J^\pi$ | $E_x$(keV) | B(GT) or B(F) |
| $1^+_1$ | 138.7 | 0.054±0.009 |
| $1^+_2$ | 232.8 | 0.014±0.002 |
| $1^+_3$ | 478.2 | 0.160±0.03 |
| $1^+_4$ | 573.0 | 0.021±0.004 |
| $1^+_5$ | 664.7 | 0.031±0.005 |
| $1^+_6$ | 1120 | ∼0.034 |
| $1^+_7$ | 1310 | ∼0.025 |
| $1^+_8$ | 1500 | ∼0.043 |
| $1^+_9$ | 1610 | ∼0.034 |
| $1^+_{10}$ | 1670 | ∼0.051 |
| $1^+_{11}$ | 1750 | ∼0.051 |
| $1^+_{12}$ | 1900 | ∼0.056 |
| $1^+_{13}$ | 2040 | ∼0.259 |
| $0^+_{IAS}$ | 15019 ± 6 | 32 |

To confirm the validity of the particle identification, we performed an additional experiment where the $^{176}$Yb target was backed with a thin mylar foil (0.086 mg/cm$^2$) to reduce the huge $^3$He$^{++} \rightarrow {}^3$He$^+$ yields. In this run, a high-resolution measurement was not possible because of the achromatic beam-transport mode. However, it was confirmed that the unresolved yield for the $1^+$ states at 195 keV and 339 keV has the same relative intensity as the summed yield for these two states in the 0° $^{176}$Yb($^3$He,$t$) spectrum taken in the dispersion-matching high-resolution mode.

To gauge the B(GT) values obtained in the ($^3$He,$t$) analysis, a calibration measurement was performed using the neighboring $^{164}$Dy($^3$He,$t$) reaction, leading to the $1^+$ ground state in $^{164}$Ho. The $^{164}$Ho ground state is known to $\beta$-decay to the $^{164}$Dy ground state with a log $ft$ value of 4.6 (Ref. [13]). This yields a B(GT) value of 0.293±0.006 for the Dy-Ho transition. The $^{164}$Dy result can thus be used to independently calibrate the strong-interaction part of the ($^3$He,$t$) reaction cross-sections for measurements on the $1^+$ states.

Fig. 1 shows the ($^3$He,$t$) spectrum on $^{176}$Yb at $\theta$=0°. We deduced the relative transition strengths of the 194.5 keV to the 338.9 keV states, by fitting the peaks with a Gaussian shape (see Fig. 1), to be 1.0:0.55. The transition strengths to the excited states were compared to that of the IAS. The excitation strengths to GT states and the IAS depend, however, on the volume integrals of the central parts of the effective interaction, $J_\tau$ and $J_{\sigma\tau}$, and distortion effects parameterized by $N_\tau^D$ and $N_{\sigma\tau}^D$ [14]. Using the observed strengths to the ground $1^+$ state and the IAS in the $^{164}$Dy($^3$He,$t$)$^{164}$Ho reaction at the same bombarding energy of 450 MeV, we calibrated the ratio of the interaction strengths including the distortion effects as

$$\frac{N_{\sigma\tau}^D|J_{\sigma\tau}|^2}{N_\tau^D|J_\tau|^2} = \frac{(\frac{d\sigma}{d\Omega})_{GT}B(F)}{(\frac{d\sigma}{d\Omega})_{IAS}B(GT)} = 7.44\pm0.79. \qquad (1)$$

Here, we used B(GT)=0.293±0.006, B(F)=N–Z=32, and $(\frac{d\sigma}{d\Omega})_{GT}/(\frac{d\sigma}{d\Omega})_{IAS}$=0.068±0.007 for the transition to the ground state of $^{164}$Ho. The value of 7.44±0.79 for the ($^3$He,$t$) reaction at 150 A·MeV agrees nicely with the values obtained by the scaling relation $[(E/A)/55MeV]^2$ which fits the systematics of (p,n) reaction data [15], and has been verified specifically for the $^{176}$Yb(p,n) reactions with values of 4.76 obtained for E$_p$=120 MeV and 8.46 for 160 MeV [9].

The present calibration method is applicable since the distortion effect and the ratio of the effective interactions $|J_{\sigma\tau}/J_\tau|$ are expected to be the same as those for the $^{176}$Yb($^3$He,$t$) reaction and the kinematic factors are cancelled out. Empirically, the volume integrals of the effective interaction and the distortion effect are not significantly different among target nuclei in the same mass region.

The B(GT) values for the $1^+$ states in $^{176}$Lu were obtained using the equation

$$B(GT) = B(F)\frac{1}{7.44}\frac{(\frac{d\sigma}{d\Omega})_{GT}}{(\frac{d\sigma}{d\Omega})_{IAS}}, \qquad (2)$$

where B(F) is (N–Z), and the ratio of $(\frac{d\sigma}{d\Omega})_{GT}/(\frac{d\sigma}{d\Omega})_{IAS}$ is obtained from the ($^3$He,$t$) spectra at 0°. The B(GT) values deduced from the 0° cross sections measured in the ($^3$He,$t$) experiment at 450 MeV are listed in Table I. The B(GT) values obtained for the possible low-lying $1^+$ levels in $^{160}$Tb from $^{160}$Gd($^3$He,$t$)$^{160}$Tb are also listed for reference. The B(GT) values for $^{176}$Yb obtained here are in agreement with the (p,n) results [9].

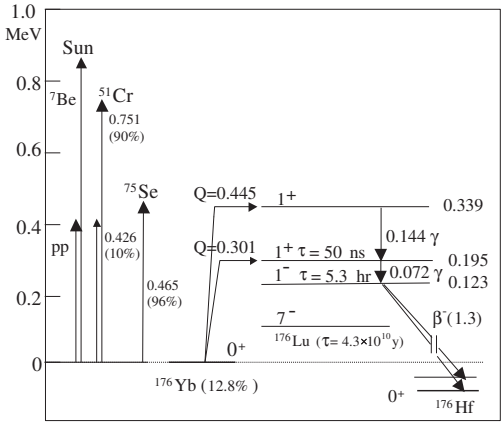


FIG. 2. Level scheme and $\gamma$-ray tags for solar neutrino detection by $^{176}$Yb. All energies are in MeV.

The reliability of the B(GT) values obtained here is supported by the following considerations: 1) scaling of reaction cross sections for GT resonances relative to the Fermi strength observed in the IAS, 2) direct use of the known $^{164}$Dy weak matrix element to calibrate the strong-interaction factor, 3) agreement of the deduced strong interaction factor with the energy scaling systematics of (p,n) reactions in general and those for $^{176}$Yb in particular, and 4) agreement of the B(GT) values obtained in the ($^3$He,$t$) and (p,n) works for $^{176}$Yb and $^{160}$Gd.

The impact of the B(GT) values for $^{176}$Yb may now be examined. The complete level scheme involved in an Yb-based detector is shown in Fig. 2. These data and those of Table I show that only the two $1^+$ levels at 194.5 keV and 338.9 keV in the final nucleus $^{176}$Lu are populated by $\nu$ capture below 3 MeV. The thresholds for $\nu$ capture are determined by the level energies and the $^{176}$Yb-$^{176}$Lu mass difference as Q($\nu$) = 301 keV and 445 keV for the above two states. The Q value of 301 keV lies below 426 keV, the endpoint of the $pp$ $\nu$ continuum. The B(GT) value for this transition is the larger of the two.

The above data on the $\nu$-capture level structure and the capture strengths establish the fundamental suitability of Yb-LENS for the long-standing problem of not only the detection but also the spectroscopy of solar neutrinos. The response of Yb-LENS to solar neutrinos, calculated for a 20 ton natural Yb target with fluxes given

by the SSM [1] is shown in Fig. 3a. The observable spectrum is that of the prompt electron $e^-$ with the energy $E_{e^-} = E_\nu$ - $Q_\nu$ that follows $\nu$-capture. Consequently, the incident $\nu_e$ spectrum is recorded directly. The principal features of the *pp*, $^7$Be, *pep* and the underlying continuum from CNO reactions in the sun are clearly resolved assuming a conservative 1 $\sigma$ energy resolution of $\Delta E/E \sim 7\%/\sqrt{E(MeV)}$.

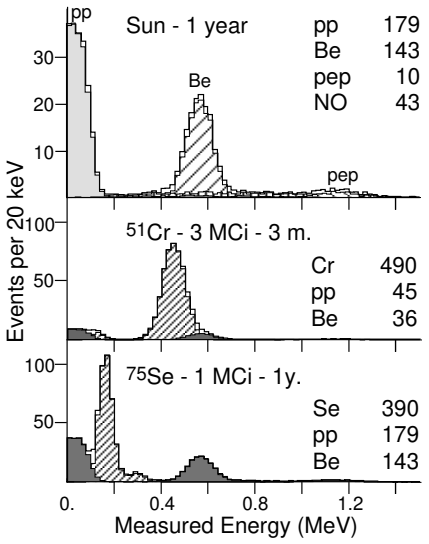


FIG. 3. Calculated $\nu_e$ spectra in a Yb-doped scintillator with a mass of 20 tons of natural Yb exposed by $\nu$'s from a) the sun, b) a radioactive source of $^{51}$Cr, and c) a source of $^{75}$Se.

Because of the importance of absolute fluxes for the three major $\nu$ sources [*pp*($E_{max}$=420 keV), $^7$Be (862 keV) and *pep* (1442 keV)] B(GT) values must be known individually for the two states in $^{176}$Lu. The simplicity of the level structure of $^{176}$Lu (only 2 states below 3 MeV) is valuable in contrast to the case of $^{160}$Gd (see Table I) in which 5 levels below 1 MeV participate and more than 13 levels below $\sim$2 MeV. Therefore, the use of Gd is less favorable than Yb since interpretation of the experimental data is more complicated besides presenting severe problems in the practical operation of the detector.

The merits of $^{176}$Yb are reinforced by plans to measure the $\nu$-absorption cross sections directly using monoenergetic $\nu$'s from megaCurie (MCi) radioactive sources. Such a calibration requires a series of sources, each with a single neutrino line, selected to discriminate level thresholds so that cross sections to individual levels can be deduced at least from the combined data. In principle, as many sources (lines) are needed as target levels revealed in this work. Clearly, such measurements are practically ruled out for Gd with so many levels to characterize. For the two levels in $^{176}$Yb, two sources are proposed. The first, $^{51}$Cr [16,17] produces a 752 keV line which populates both the Yb transitions (the weaker line at 426 keV produces a much weaker signal). The second source, $^{75}$Se [18,19] produces a line at 465 keV which is sensitive only to the lower level. Figs. 3b and c depict the LENS response for these two calibration lines. They show that the neutrino response of an Yb-LENS can be calibrated experimentally without interference from a "background" of solar neutrinos.

In summary, we report experimental results on the Gamow-Teller transitions from $^{176}$Yb to $^{176}$Lu using the ($^3$He,$t$) reaction at $E(^3\mathrm{He})$=450 MeV. A high-resolution measurement enabled us to resolve the low-lying $1^+$ states in the residual nucleus. By taking the ratios of the excitation strengths for the IAS and the Gamow-Teller states, we deduce the B(GT) values for low-lying $1^+$ states after calibrating the reaction mechanism. The data establish the foundations for a practical real-time $^{176}$Yb detector for sub-MeV solar $\nu$'s including *pp* $\nu$'s. Solar $\nu$ absorption rates for a 20-ton Yb detector are given together with those for the $^{51}$Cr and $^{75}$Se $\nu$ calibrations.

The authors acknowledge the RCNP cyclotron staff for their support during the experiment. The present work has been supported by the Ministry of Education, Science, Sports and Culture (Monbusho) with Grant No. 09041108 and by the Japan Society for the Promotion of Science (JSPS).

[1] J. N. Bahcall, Nucl. Phys. **B 77**, 64 (1999).
[2] T.A. Kirsten, Nucl. Phys. **B 77**, 26 (1999).
[3] V.N. Gavrin, Nucl. Phys. B **77**, 20 (1999).
[4] Y. Fukuda *et al.,* Phys. Rev. Lett. 81, 1158 (1998).
[5] Y. Fukuda *et al.,* Phys. Rev. Lett. 81, 1562 (1998).
[6] C. Arpesella et al., "Borexino: A real time detector for low energy solar neutrinos", Ed. G. Bellini and R.S. Raghavan, INFN-Milano (unpublished) (1991).
[7] R.S. Raghavan, Phys. Rev. Lett. **78**, 3618 (1997).
[8] Letter of Intent to LNGS on "LENS" (Low Energy Neutrino Spectroscopy) January 1999.
[9] M. Bhattacharya *et al.,* submitted to Phys. Rev. Lett.
[10] M. Fujiwara *et al.,* Nucl. Phys. A **599**, 223c (1996).
[11] M. Fujiwara *et al.,* Nucl. Instr. Meth. Phys. Res. A **422**, 484 (1999).
[12] K. Dennis *et al.,* Phys. Rev. A **50**, 3992 (1994).
[13] E.N. Shurshikov and N.V. Timofeeva, Nuclear Data Sheets **65**, 365 (1992).
[14] C.D. Goodman *et al.,* Phys. Rev. Lett. **44**, 1755 (1980).
[15] C.D. Goodman, Nucl. Phys. A **577**, 3c (1994).
[16] R.S. Raghavan, Proc. Conf. on "Status and Future of solar neutrino research", Brookhaven National Laboratory, 1978, BNL-50879, Vol II, p. 270 (unpublished).
[17] M. Cribier *et al.,* Nucl. Instr. Meth. Phys. Res. A **378**, 233 (1996).
[18] J-F Cavaignac and M. Cribier, private communication.
[19] V.N. Kornoukhov *et al.,* ITEP Preprint 18-99, Inst. Theoretical and Exp. Physics, (1999).